

# Human and Ecological Risk Assessment: An International Journal

ISSN: 1080-7039 (Print) 1549-7860 (Online) Journal homepage: <http://www.tandfonline.com/loi/bher20>

## Predictive Ecological Modeling of Harmful Algal Blooms

John J. Walsh , Bradley Penta , Dwight A. Dieterle & W. Paul Bissett

To cite this article: John J. Walsh , Bradley Penta , Dwight A. Dieterle & W. Paul Bissett (2001) Predictive Ecological Modeling of Harmful Algal Blooms, Human and Ecological Risk Assessment: An International Journal, 7:5, 1369-1383, DOI: [10.1080/20018091095069](https://doi.org/10.1080/20018091095069)

To link to this article: <https://doi.org/10.1080/20018091095069>



Published online: 03 Oct 2012.



Submit your article to this journal [↗](#)



Article views: 146



View related articles [↗](#)



Citing articles: 30 View citing articles [↗](#)

## Predictive Ecological Modeling of Harmful Algal Blooms

John J. Walsh,<sup>1,\*</sup> Bradley Penta,<sup>1</sup> Dwight A. Dieterle,<sup>1</sup> and W. Paul Bissett<sup>2</sup>

<sup>1</sup>College of Marine Science, University of South Florida, 140 Seventh Avenue South, St. Petersburg, FL 33701. <sup>2</sup>Florida Environmental Research Institute, 4807 Bayshore Boulevard, Suite 101, Tampa, FL 33611

### ABSTRACT

We have thus far constructed a series of coupled ecological/physical models to predict the origin and fate of harmful algal blooms of the toxic dinoflagellate, *Gymnodinium breve*, on the West Florida shelf. We find that (1) the maximal population growth rate of *G. breve* must be  $\sim 0.80 \text{ day}^{-1}$  during initiation of a red tide, but as little as  $0.08 \text{ day}^{-1}$  during its decay, (2) diatoms dominate when estuarine and shelf-break supplies of nitrate are made available to a model community of small and large diatoms, coccoid cyanophytes and *Trichodesmium*, non-toxic and red-tide dinoflagellates, microflagellates, and coccolithophores, (3) a numerical recipe for large red tides of *G. breve* requires DON supplies, mediated by iron-starved, nitrogen-fixers, while small blooms may persist on sediment sources of DON, (4) selective grazing must be exerted on the non-toxic dinoflagellates, and (5) vertical migration of *G. breve* in relation to seasonal changes of summer downwelling and fall/winter upwelling flow fields determines the duration and intensity of red tide landfalls along the barrier islands and beaches of the west coast of Florida, once other losses are specified.

Given poorly known initial and boundary conditions and the expense of ship-board monitoring programs, however, bio-optical moorings or remote sensors are the most likely sources of model validation and improved HAB forecasts. Accordingly, the bio-optical implications of our ecological models must be included in future simulation analyses of HABs on both the West Florida shelf and within other coastal regions. Of particular importance for initiation of the coupled biophysical models is an improved understanding of the relationship of remotely sensed surface signals to shade-adapted dinoflagellates, aggregating below the first optical depth of the water column.

---

\* Corresponding author.

**Key Words:** algal blooms, red tides, ecological models, *Gymnodinium breve*, dinoflagellates, HAB forecast.

## INTRODUCTION

The first written record of a red tide in the eastern Gulf of Mexico was provided in 1542 by A.N. Cabeza de Vaca. At that time, predictive models of the consequences of such a harmful algal bloom (HAB) consisted of “the oyster is unseasonable and unwholesome in all months that have not the letter ‘r’ in their name” (Buttes 1599). Since the greatest numbers of large red tides ( $>0.5 \times 10^6$  cells  $l^{-1}$ ) over the last 40 years have occurred during both September and October along the west coast of Florida; however, the utility of such generic prognostic models is marginal at best!

Upon identification of *Gymnodinium breve* as the causative agent of most Florida red tides (Davis 1948), a simple model of phytoplankton growth and lateral mixing was developed (Kierstead and Slobodkin 1953; Slobodkin 1953) for analysis of the 1947 red tide caused by *G. breve* (Gunther *et al.* 1948). At a net realized growth rate of  $\sim 0.3 \text{ day}^{-1}$  for this particular toxic dinoflagellate and a mixing coefficient of  $1 \times 10^6 \text{ cm}^2 \text{ sec}^{-1}$ , one might conclude that only patch sizes of  $>12 \text{ km}$  radii may persist, despite observations of phytoplankton blooms at much smaller length scales (Franks 1997). While more complex circulation models have subsequently been applied to other HAB systems (Yanagi *et al.* 1995; Joint *et al.* 1997), none have really addressed the difficult question of HAB origin in an ecological context. Specification of the reasons — and thus the structure of a numerical model — for successful competition by toxic species requires, of course, an answer to Hutchinson’s (1961) paradox of the plankton, with its implied absence of competitive exclusion among phytoplankton communities.

We have thus far constructed a series of 1-dimensional and 3-dimensional ecological models (Figure 1), embedded in circulation models of varying complexity, to predict the origin and fate of HABs of *G. breve* on the West Florida shelf. A traditional N-P-Z [Nutrient-Phytoplankton - Zooplankton] model with one state variable each to represent the plant and animal communities of oceanic waters is incapable of addressing complex ecosystems of the coastal zone, where most HABs now prevail (Tester and Steidinger 1997; Steidinger *et al.* 1998). Some of the numerical results from our ECOHAB [Ecology and Oceanography of Harmful Algal Blooms]:Florida project are presented here. They highlight our findings about the specific niche this red tide organism occupies, during seasonal transitions of nutrient supply and circulation patterns on the West Florida shelf. Any numerical model, of course, represents a series of hypotheses, drawn from prior observations, which were the thrust of our retrospective simulation analyses to test the following eight assumptions.

Based on Loop Current influxes of nitrate from the shelf-break during USFWS [United States Fish and Wildlife Service] cruises in 1958 to 1961 (Dragovich *et al.* 1961;1963) and estuarine discharges of this form of nitrogen from the Apalachicola and Suwanee Rivers during FMRI [Florida Marine Research Institute] Coastal Production cruises in 1992-1993 (Gilbes *et al.* 1996), we postulated that (1) diatoms outcompete the other functional groups of phytoplankton (Figure 1) during spring. Fallout of the poorly-grazed spring bloom of diatoms (Hitchcock *et al.* 2000) during

# Ecological Modeling of Harmful Algal Blooms

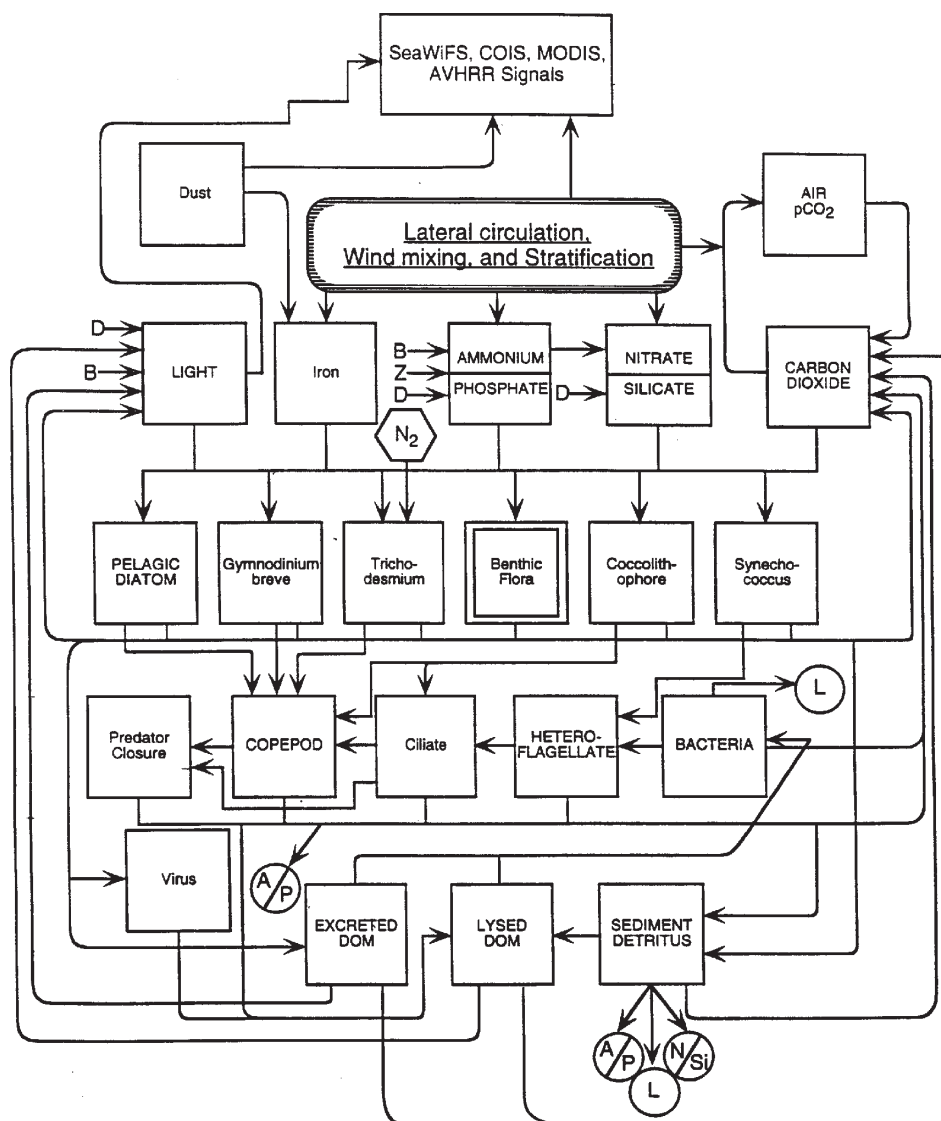


**Figure 1.** State variables of an ecologically complex numerical food web, coupled to a POM model of water circulation, for analysis of phytoplankton competition leading to a harmful algal bloom (HAB) of *Gymnodinium breve* on the West Florida shelf.

the 1996 Florida Shelf Lagrangian Experiment suggests (2) sequestration of remineralized ammonium by benthic microflora, rather than subsequent sediment effluxes for support of another spring bloom in the water column, except for episodic resuspension events. Such an indirect nutrient loading (3) triggers sixfold seasonal increments of sediment chlorophyll here (G. Vargo, personal communication) and on the Georgia shelf (Nelson *et al.* 1999), possibly conditioning organic sources of nutrients for red tides later in summer and fall on the Florida shelf.

During the FMRI cruises in 1965, 1966, and 1976, blooms of *Trichodesmium* also preceded those of toxic and edible dinoflagellates on the West Florida shelf. In response to alleviation of summer Fe-limitation by atmospheric supplies of Saharan dust (Walsh and Steidinger 2001) (4) excretion of DON by these nitrogen-fixers (Glibert and Bronk 1994; Lenos *et al.* 2001) may fuel the subsequent fall dinoflagellates blooms — at least the large ones. Tenfold variation of copepod grazers from one year to the next (Houde and Chitty 1976) would lead (5) to selective grazing pressure (Kleppel *et al.* 1996; Turner and Tester 1997) on the other dinoflagellates, ensuring blooms of the slower growing, toxic *Gymnodinium breve*, when copepods are abundant.

Once red tides are established, vertical movements of *G. breve* (Heil 1986; Kamykowski *et al.* 1998) in relation to stratification of the water column (6) determine whether near-bottom or near-surface populations are entrained by onshore currents. Concurrent CZCS imagery and FMRI cruises (Haddad 1982) suggest that (7) an upwelling circulation mode and an offshore source of *G. breve* in fall 1979 led to a red tide near the coast. Finally, biomass of all the smaller size classes of phytoplankton may be held down by grazing stresses of the heterotrophic flagellates and ciliates (Fahnenstiel *et al.* 1995; Strom and Strom 1996), who may also eat *G. breve* (Hansen 1995; Nakamura *et al.* 1996), with (8) occasional blooms of the microflagellates (Figure 1) stimulated by prey-switching of copepods to the larger ciliates, but not to the smaller heterotrophic flagellates.

## METHODS

We deal with the bewildering complexity of the “real world” HABs by construction of a series of perhaps similarly opaque biological models, driven by physical ones of varying sophistication. At one extreme, our 3-dimensional application of the Princeton Ocean Model (POM) employs a topography-following sigma coordinate system over 16 levels in the vertical dimension, a curvilinear coordinate system in the horizontal, and an embedded Mellor-Yamada turbulence closure scheme for determining vertical mixing, to compute the time-dependent, barotropic flow fields at ~10-km resolution of the whole West Florida shelf (Li and Weisberg 1999). The coupled biological model then considers an initial condition of a mature HAB of ~10 mg chl m<sup>-3</sup> of *G. breve*, simply growing at net rates of either 0.15 day<sup>-1</sup> or 0.80 day<sup>-1</sup> in the absence of competition. Various light-regulated cases of either implicit or no nutrient-depletion, and presence or absence of both convective mixing and vertical migration are explored, but no grazing or photolytic losses are applied within a fall water column (Walsh *et al.* 2001a).

In contrast, the 1-dimensional cases of spring nitrate supply and summer DON sources assume a constant density profile over the 40-m isobath, above which only vertical mixing of the phytoplankton community occurs under constant wind forcing and no advection. Over the 60 day periods after nutrient injection to a background HAB of ~0.03 mg chl m<sup>-3</sup> (or  $3 \times 10^3$  cells l<sup>-1</sup>) of *G. breve*, growing at a maximal gross rate of ~0.80 day<sup>-1</sup>, competition is now effected by light regulation (via the separate saturation, specific absorption and C/chl parameters), explicit nutrient limitation (via Michaelis half-saturation parameters), varying respiration rates, and differential grazing stresses among eight functional groups ( $P_i$ ) of phy-

# Ecological Modeling of Harmful Algal Blooms

toplankton (Table 1). For example, the small and large diatoms sink as a function of their biomass aggregations (Walsh and Dieterle 1994), the microflagellates and coccoid cyanophytes are neutrally buoyant, the non-toxic dinoflagellates and the *G. breve* HABs migrate, *Trichodesmium* is positively buoyant, and the coccolithophores sink at a constant rate of 1.5 m day<sup>-1</sup> (Table 1).

Following competition theory (*e.g.*, Huisman and Weissing 1999), our limiting resources of light (I), nitrate, ammonium, DON, phosphate, DOP, iron, and silicate

**Table 1. Competition parameters of functional groups of phytoplankton in relation to grazing stress effected by their predators, macrozooplankton (MZ) and protozoans (PN), during an annual cycle of thermal-modulated (15°C to 30°C) growth on the West Florida shelf.**

	Small diatom	Large diatom	<i>G. breve</i>	Other dino- flagellate	Coccolith- ophore	μflag- ellate	<i>Tricho- desmium</i>	<i>Synechco- coccus</i>
Diameter (μm)	8	50	25	25	6	2	10	0.8
w <sub>s</sub> (m day <sup>-1</sup> )	[biomass] <sup>2</sup>		+ 1 m hr <sup>-1</sup>	± 2 m hr <sup>-1</sup>	1.5	0.0	± 1.5 m hr <sup>-1</sup>	0.0
μ <sub>max</sub> (day <sup>-1</sup> @ 10°C)	0.6	0.5	0.2	0.3	0.9	0.5	0.2	0.5
μ <sub>max</sub> (day <sup>-1</sup> @ 20°C)	1.2	1.0	0.4	0.6	1.9	0.9	0.4	1.0
μ <sub>max</sub> (day <sup>-1</sup> @ 30°C)	2.4	2.0	0.8	1.2	0.6	1.8	0.8	2.0
I <sub>sat</sub> (μE m <sup>-2</sup> sec <sup>-1</sup> )	190	190	65	150	425	275	300	125
k <sub>nitrate</sub> (μmol l <sup>-1</sup> )	0.4	1.7	0.5	1.8 (+ dark)	0.2	0.2	--	0.2
k <sub>ammonium</sub> (μmol l <sup>-1</sup> )	1.0	2.0	0.5	0.9	0.1	0.2	--	0.1
k <sub>DON</sub> (μmol l <sup>-1</sup> )	8.5	10.0	1.0	3.0	--	--	--	--
k <sub>phosphate</sub> (μmol l <sup>-1</sup> )	0.4	0.6	0.2	0.2	0.1	0.3	9.0	2.0
k <sub>DOP</sub> (μmol l <sup>-1</sup> )	--	--	1.0	1.0	--	--	1.0	--
k <sub>iron</sub> (nmol l <sup>-1</sup> )	0.1	0.3	0.2	0.2	0.01	0.06	1.0	0.03
k <sub>silicate</sub> (μmol l <sup>-1</sup> )	0.8	1.5	--	--	--	--	--	--
r <sub>i</sub> (% μ <sub>max</sub> )	10	10	25	25	10	15	50	10
p <sub>i</sub> (% MZ or PN)	60MZ+10PN 40MZ		1MZ	20MZ+5PN	20MZ+60PN	15MZ+90PN	10MZ	100PN
k <sub>p</sub> (10 <sup>-2</sup> mg <sup>-1</sup> chl m <sup>2</sup> )	4.8	2.3	3.5	4.8	4.8	5.7	4.8	6.5
C cell <sup>-1</sup> (pg)	32	1750	300	600	18	6	200	0.06
C/chl (pg pg <sup>-1</sup> )	55	45	30	100	75	100	200	30
N/P/Fe (molar)	15/1/.003	15/1/.003	15/1/.03	15/1/.03	15/0.5/.001	15/1/.001	15/0.5/.03	15/1/.001

should allow the coexistence of eight functional groups of phytoplankton. For numerical reasons (Walsh 1975), we provide small refugia for each population, such that Hutchinson's paradox is moot — in these simulation runs, iron is also an implicit variable, setting the rate of DON released during nitrogen-fixation of different scenarios. To conserve space in this short communication, we refer discussion of the partial differential equations for each state variable ( $u$ ,  $v$ ,  $w$ ,  $I$ ,  $\text{NO}_3$ ,  $\text{NH}_4$ ,  $\text{DON}$ ,  $\text{PO}_4$ ,  $\text{DOP}$ ,  $\text{Fe}$ ,  $\text{SiO}_4$ ,  $\text{P}_{1-8}$ , protozoans, and copepods) and their numerical solution to prior publications (Walsh and Dieterle 1994; Li and Weisberg 1999; Bissett *et al.* 1999a, b; Walsh *et al.* 1999; Walsh *et al.* 2001b; Yang and Weisberg 1999; Penta 2000).

## RESULTS

The 1-d model results of nutrient limitation, light regulation, and differential grazing at the 40-m isobath (Penta 2000) suggest that in response to both estuarine and Loop Current nutrient loadings to the northwest Florida shelf, small and large diatoms first outcompete other taxa with a yield of  $\sim 3.2 \text{ mg chl m}^{-3}$  (Figure 2a). They emerge from an initial phytoplankton field of other competing functional groups of *G. breve*, the non-toxic dinoflagellates, chlorophytes, coccolithophores, diazotrophs — *e.g.* *Trichodesmium*, and *Synechococcus*, if the N/P ratios of the nutrient supply approximate the Redfield ratio of phytoplankton biomass. In the Apalachicola River scenario of a near-surface loading of  $5.0 \text{ NO}_3 + 0.1 \text{ NH}_4 + 0.0 \text{ DON}$ ,  $0.25 \text{ PO}_4 + 0.15 \text{ DOP}$ , and  $15.0 \text{ SiO}_4 \text{ mmol m}^{-3}$ , the computed biomass of all phytoplankton is  $4.5 \text{ mg chl m}^{-3}$  after a week (Figure 2a), as observed during the FMRI cruise in 1992 and by CZCS imagery (Gilbes *et al.* 1996), with a simulated productivity pulse of  $\sim 500 \text{ mg C m}^{-2} \text{ day}^{-1}$  (Figure 2b). After nutrient depletion of surface waters and diurnal upward movement of *G. breve*, their maximal simulated stocks are only  $2.5 \text{ mg chl m}^{-3}$  by day 60, however, such that tenfold larger populations of the real world HABs (Carder and Steward 1985; Vargo *et al.* 1987; Walsh and Steidinger 2001) require additional nutrient supplies.

In a 1-d model case of nitrogen-limited waters between Tampa Bay and Charlotte Harbor, with a total N/P loading ratio of 0.45, a supply of both DON from iron-replete nitrogen-fixers and of  $\text{DOP/PO}_4$  from the Peace/Alafia River estuaries first yields a combined diatom stock of  $< 0.4 \text{ mg chl m}^{-3}$  after 5 days (Figure 3a), with a minimal pulse of net photosynthesis of  $\sim 200 \text{ mg C m}^{-2} \text{ day}^{-1}$  (Figure 3b). Yet, once *Trichodesmium* accumulates a biomass of  $> 5 \text{ mg chl m}^{-3}$  on day 40, releasing as much as  $3 \text{ mmol DON m}^{-3}$  in the model, and the more palatable, non-toxic dinoflagellates are preferentially consumed, *G. breve* dominate. By day 60, they have a subsurface biomass of  $\sim 40 \text{ mg chl m}^{-3}$ , *i.e.*, as measured both previously above the 20-m isobath during October 1986 (Walsh and Steidinger 2001) and more recently in October 1999 and 2000 during ECOHAB:Florida cruises. Simulated primary production then amounts to  $\sim 800 \text{ mg C m}^{-2} \text{ day}^{-1}$  (Figure 3b).

With a maximal growth rate of  $0.80 \text{ day}^{-1}$  for *G. breve* (Table 1), light and nutrient limitation forced a realized gross growth of  $\sim 0.30 \text{ day}^{-1}$  over 60 days in the model — before a respiration loss of 25% (Table 1). The mean computed net value of  $\sim 0.23 \text{ day}^{-1}$  is thus similar to those of  $0.25 \text{ day}^{-1}$  estimated for the 1980 red tide (Walsh and Steidinger 2001) and of  $0.27 \text{ day}^{-1}$  measured for the 1996 red tide (Van Dolah and



# Ecological Modeling of Harmful Algal Blooms

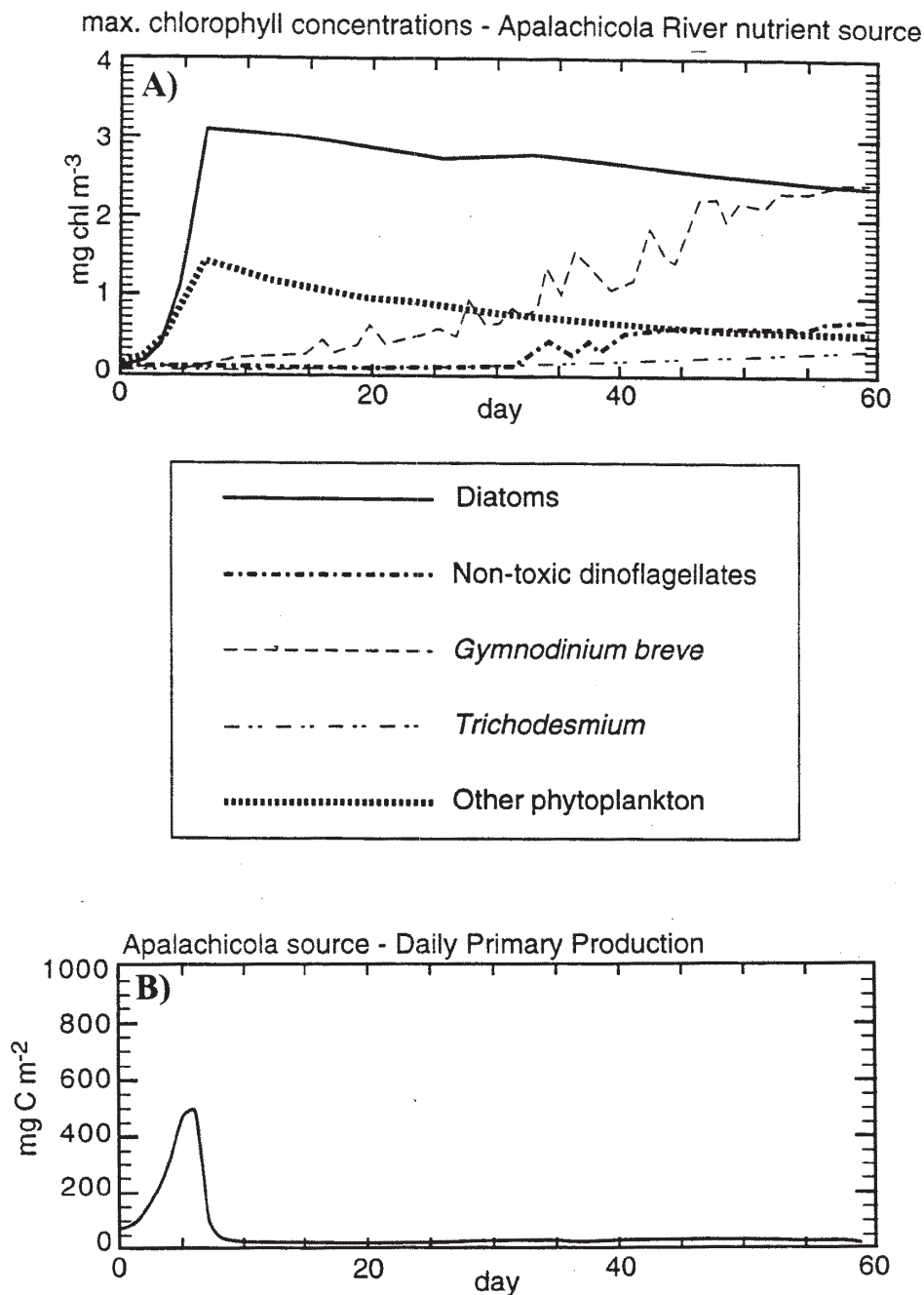


Figure 2. The simulated daily phytoplankton responses during HAB initiation to a total spring estuarine N/P loading ratio of 12.75, with respect to both (A) maximal biomasses (mg chl m<sup>-3</sup>) within a 40-m water column of the functional groups of small + large diatoms, *Trichodesmium spp.*, non-toxic dinoflagellates, *G. breve*, the sum of coccolithophores + chlorophytes + *Synechococcus*, and (B) the daily community primary production (mg C m<sup>-2</sup>).



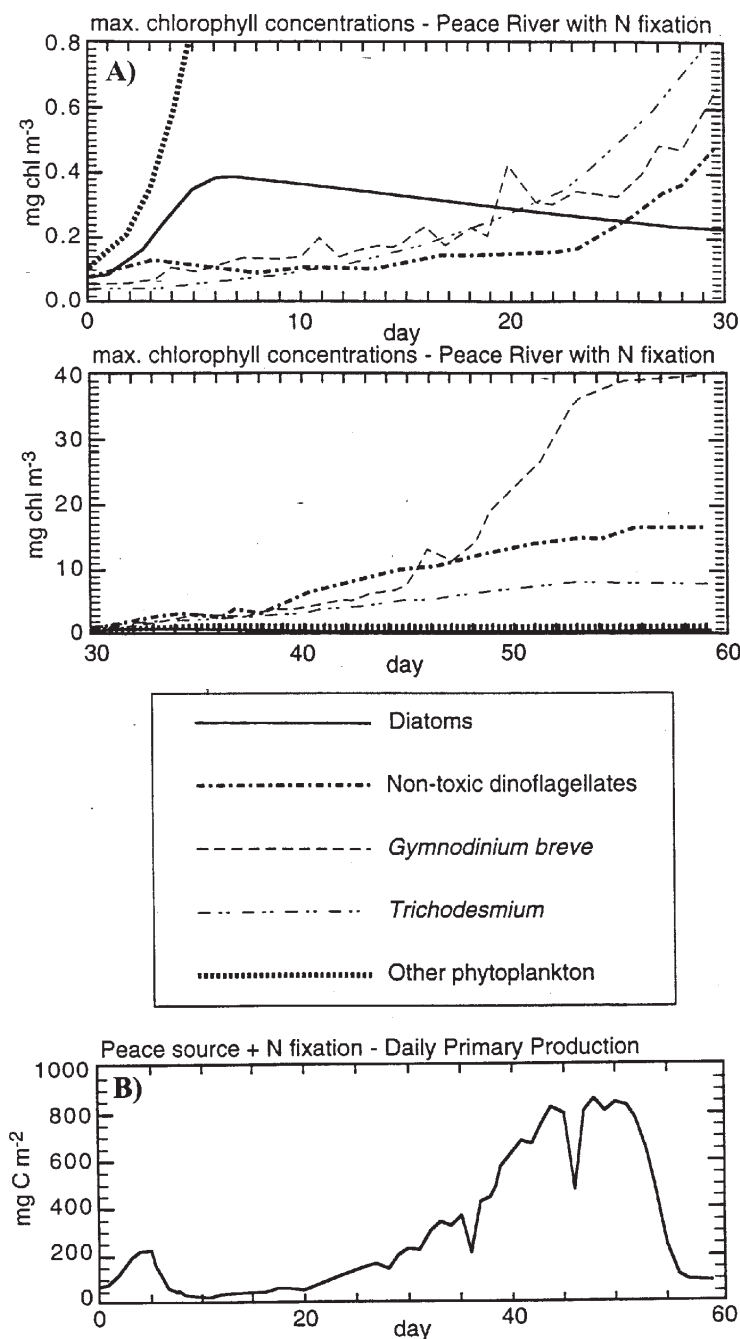


Figure 3. The simulated daily phytoplankton response during HAB initiation to a total summer estuarine N/P loading ratio of 0.45, together with iron-replete nitrogen-fixation, with respect to both (A) maximal biomasses (mg chl m<sup>-3</sup>) within a 40-m water column of the functional groups of small + large diatoms, *Trichodesmium* spp., *G. breve*, non-toxic dinoflagellates, the sum of coccolithophores + chlorophytes + *Synechococcus*, and (B) the daily community primary production (mg C m<sup>-2</sup>). Note the scale change on the second half of panel A.

Leighfield 1999). Note that this is the realized population growth rate of a young *G. breve* HAB, subjected to no other losses from any microbial, protozoan, or crustacean predators.

Assuming  $1 \text{ mg chl m}^{-3} = 1 \times 10^5 \text{ } G. \text{ breve cells l}^{-1}$  for laboratory cultures (Shanley and Vargo 1993), as also found for field populations in October 1976 (Walsh and Steidinger 2001), the HAB biomass was  $\sim 10 \text{ mg chl m}^{-3}$  at one station above the  $\sim 30\text{-m}$  isobath, north of Tampa Bay, during the 5 to 6 December 1979 red tide (Figure 4a). Repeated shipboard and helicopter observations of this time series show a southward movement of this patch by 19 to 21 December 1979 (Figure 4b), as also suggested by concurrent CZCS imagery, with  $>5 \text{ mg chl m}^{-3}$  of *G. breve* then found south of Tampa Bay (Walsh *et al.* 2001a). Additional red tide samples were collected at 25 coastal sites, on barrier islands and within their passes, during 1979 to 1980 along the west coast of Florida (Figure 4).

A mature HAB of  $\sim 10 \text{ mg chl m}^{-3}$  was released uniformly over depth above the  $\sim 30\text{-m}$  isobath on 25 November (dotted contours of Figure 5) in the POM of the West Florida shelf (Walsh *et al.* 2001a). To allow for nutrient depletion in offshore waters after HAB development, a light-regulated net growth rate of  $0.15 \text{ day}^{-1}$  was first applied to *G. breve* populations, migrating upwards at  $1 \text{ m hr}^{-1}$  under light intensities of  $\leq 65 \text{ uE m}^{-2} \text{ sec}^{-1}$  and subjected to nocturnal convective mixing. Driven by observed winds at the Tampa airport, the trajectory of the simulated patch at a depth of  $0.5 \text{ m}$  on 5 and 20 December (Figures 5a, b) matches the observed one along this isobath (Figure 4), if one samples the near-surface distribution of *G. breve* biomass at sunrise.

At midday, noon surface incident radiation of  $1200 \text{ uE m}^{-2} \text{ sec}^{-1}$  in the model forces the red tide to then aggregate at a depth of  $10 \text{ m}$  within a subsurface maximum of  $\sim 20 \text{ mg chl m}^{-3}$  by 20 December, compared to surface populations of  $<0.1 \text{ mg chl m}^{-3}$ . Convective mixing between midnight and 0600 leads to simulated surface stocks of  $>5 \text{ mg chl m}^{-3}$  to the north of Tampa Bay on 5 December (Figure 5a) and to the south on 20 December (Figure 5b) — as observed. The same vertical profiles of *G. breve* were also found on the West Florida shelf at 0600 [homogeneous] and 1400 [subsurface maximum] on 11 to 12 September 1980 (Heil 1986).

With no vertical migration and a net growth rate of  $0.80 \text{ day}^{-1}$  in a second case study, however, the model's surface populations did not replicate the observations - they were instead advected farther offshore to the  $50\text{-m}$  isobath by the 5th and to the  $200\text{-m}$  isobath by the 20th of December within the surface Ekman layer of POM. Furthermore, the computed surface stock of *G. breve* on 20 December in this second scenario was a maximum of  $\sim 180 \text{ mg chl m}^{-3}$ , almost 20-fold that observed (Figure 4b).

In terms of the amount and timing of the red tide washed ashore in the model by 18 December, a third scenario of a migrating population of *G. breve* with the larger growth rate of  $0.80 \text{ day}^{-1}$  more closely matched the observed red tide initially encountered at the 25 sites within nutrient-rich coastal waters — compared to scenarios of the smaller growth rate. Once more, however, continued increments of the faster-growing *G. breve* by 28 December then led to simulated stocks of  $\sim 400 \text{ mg chl m}^{-3}$  in the model -  $>20\text{-fold}$  greater than those usually observed, except in bays (Millie *et al.* 1997) of limited flushing.

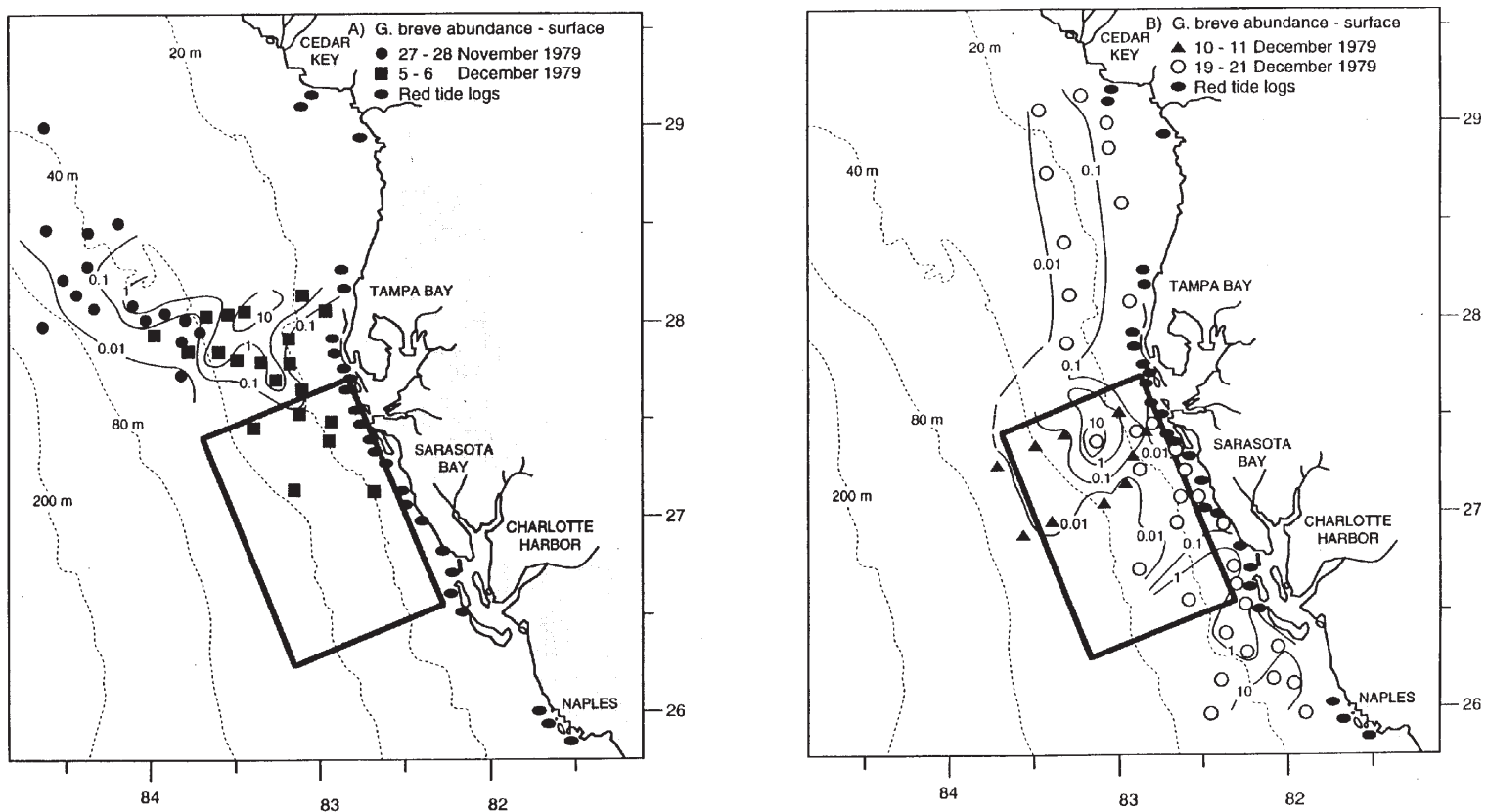


Figure 4. Surface observations of *G. breve* abundance ( $10^5$  cells  $l^{-1}$ ) during A) 27-28 November 1979 (●)/5-6 December 1979 (■) and B) 10-11 December 1979 (▲)/19-21 December 1979 (○) in relation to both red tides sampled on piers and bridges during 11/25/79-2/8/80 and to the present ECOHAB:Florida control volume (▢) bounded by ADCP arrays on the West Florida shelf.

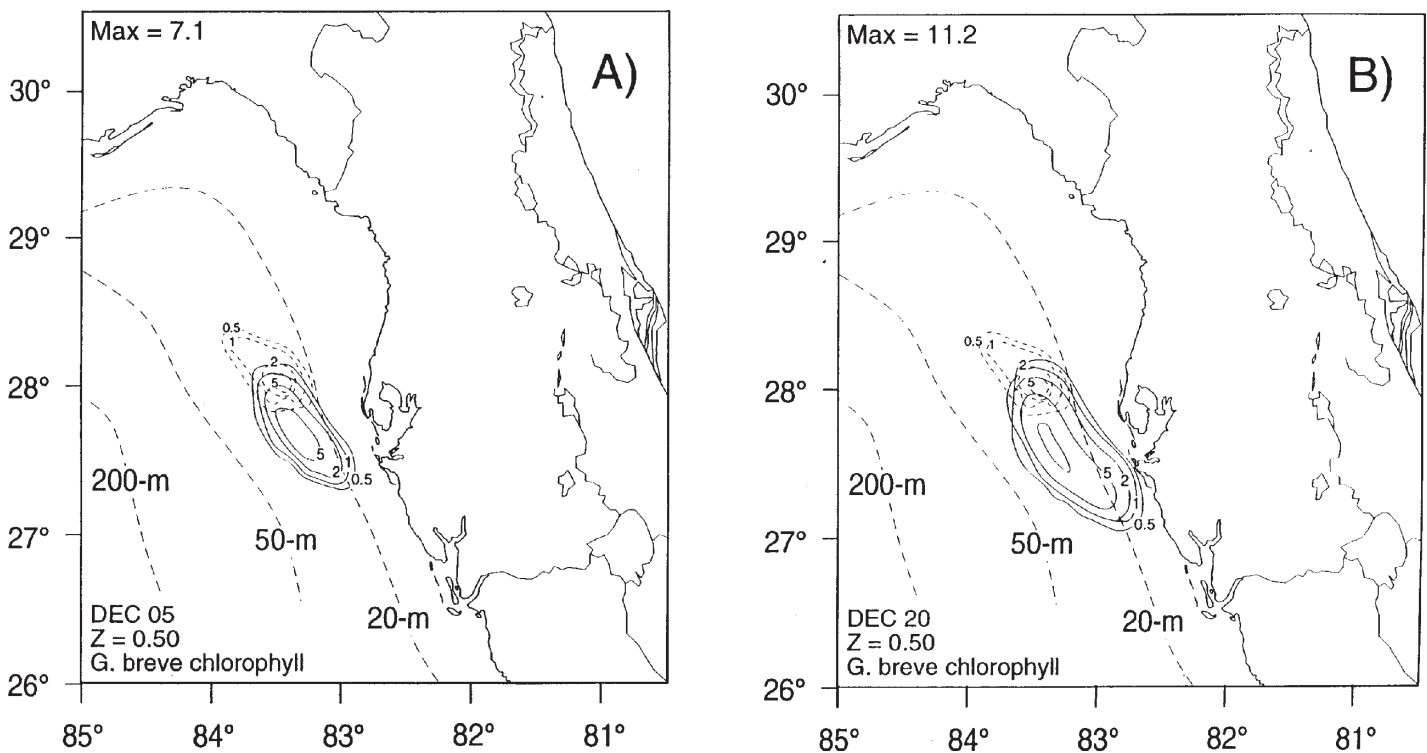


Figure 5. The simulated daily trajectory of a near-surface mature red tide ( $10^5$  cells  $l^{-1}$  = 1 mg chl  $m^{-3}$ ) of *G. breve*, growing at a net rate of  $\sim 0.15$  day $^{-1}$  with vertical migration and nocturnal convective mixing, during sunrise (0600 hr) on A) 5 December and B) 20 December 1979, after HAB initiation on 25 November (--- contours) at the  $\sim 30$ -m isobath and under forcing of POM by winds measured at the Tampa International Airport.

Since net population growth rates of 0.25 to 0.27 day<sup>-1</sup> are found for field populations of *G. breve* in nearshore waters off the Florida west coast (Van Dolah and Leighfield 1999; Walsh and Steidinger 2001), similar to the net growth rates of 0.15 to 0.23 day<sup>-1</sup> employed in some cases of the 1-d and 3-d models, the higher apparent net growth rate of 0.80 day<sup>-1</sup> - required to match coastal observations - is not a biological one. It must instead reflect physical accumulation of *G. breve* at nearshore fronts, not resolved by the barotropic version of POM. Furthermore, once a red tide is both grown and physically concentrated, some unknown time-dependent losses on the West Florida shelf — such as cumulative UV photo-inhibition, biomass-dependent viral/bacterial lysis, non-selective grazing by copepods, tintinnids, and heterotrophic dinoflagellates, and physical dispersion — must curtail the mature HABs, in contrast to the developing ones.

## DISCUSSION

If the water does not move on the West Florida shelf, and we specify delivery of DON to toxic dinoflagellates, such that diatoms can not access this resource and their other competitors are grazed, a HAB of *G. breve* is formed in our 1-d model. Once such a HAB is formed and the water does move, we can also predict its alongshore transport and landfall with our 3-d model. Thus far, however, we have not explicitly simulated the processes over time and space that lead to formulation of a Florida HAB in the “real world”, after DON is released somewhere on the shelf by diazotrophs in response to Saharan dust storms, or by bacteria in response to decay of near-bottom diatom blooms, derived from prior estuarine or Loop Current pulses of nitrate.

Important details remain to be included in the next version of the coupled biophysical models. For example, CDOM may serve as a sun screen in coastal waters and *G. breve* prefers bacterial-mediated ammonium (Steidinger *et al.* 1998), rather than the precursor amino acids (Baden and Mende 1979), released by *Trichodesmium* (Capone *et al.* 1994). Bacteria, DOC, and CDOM must thus be added as explicit variables (Walsh *et al.* 1999; 2001b), as well as iron (Leonard *et al.* 1999), in a more sophisticated model of microbial competition (Morin 2000). Phytoplankton must be grazed uniformly by imprudent protozoans (Hansen 1995; Nakamura *et al.* 1996) and subjected to UV-B radiation (Millie, *et al.* 1995). Such competition must also invoke internal cell quotas and changing particulate ratios (*e.g.* Bissett *et al.* 1999a) of carbon, nitrogen, phosphorus, silicon, and iron. Finally, a time-dependent baroclinic mode must be added to POM at ~1-km resolution, for correct depiction of summer flows and frontal features on this shelf (Yang and Weisberg 1999).

Additional biochemical and physical variables for the next coupled HAB model may not be sufficient, because the initial and boundary conditions will always be poorly known. Like models of the weather on land, predictive HAB models must be continually validated with data, to correct for the poor knowledge of pre-HAB conditions. However, satellite color data do not provide initial conditions for harmful algal blooms of shade-adapted species, found below the first optical depth of offshore source regions.

Within nearshore waters, SeaWiFS and MODIS products may eventually provide validation data on large red tides, once contaminations from CDOM, suspended

## Ecological Modeling of Harmful Algal Blooms

sediment, and bottom reflectance are removed. Accordingly, the biooptical implications of our ecological models (Bissett *et al.* 1999b; Schofield *et al.* 1999) must be included in future simulation analyses of HABs to interpret surface signals of migrating, shade-adapted *G. breve* populations.

### ACKNOWLEDGMENTS

This analysis was funded by grants NA76RG0463 and NA96OP0084 from the National Oceanic and Atmospheric Administration to JJW, NAG5-6449 to JJW from the National Aeronautics and Space Administration, as well as N00014-96-1-5024 and N00014-99-1-0212 to JJW, and N00014-98-1-0844 to WPB from the Office of Naval Research. We also thank the State of Florida and EPA grant R 827085-01-0 for support of the field work by other PIs of the ECOHAB:Florida program. This is ECOHAB contribution # 18.

### REFERENCES

- Baden DG and Mende TJ. 1979. Amino acid utilization by *Gymnodinium breve*. *Phytochemistry* 18:247-51
- Bissett WP, Walsh JJ, Dieterle DA, *et al.* 1999a. Carbon cycling in the upper waters of the Sargasso Sea. I. Numerical simulation of differential carbon and nitrogen fluxes. *Deep-Sea Res* 46:205- 69
- Bissett WP, Carder KL, Walsh JJ, *et al.* 1999b. Carbon cycling in the upper waters of the Sargasso Sea. II. Numerical simulation of apparent and inherent optical properties. *Deep-Sea Res* 46:273-320
- Buttes H. 1599 Dyets dry dinner - see Schofield *et al.* 1999
- Capone DG, Ferrier MD, and Carpenter EJ . 1994. Amino acid cycling in colonies of the planktonic marine cyanobacterium *Trichodesmium thiebautii*. *Appl Envir Microbiol* 60:3989-95
- Carder KL and Steward RG. 1985. A remote-sensing reflectance model of a red-tide dinoflagellate off west Florida. *Limnol Oceanogr* 30:286-98
- Davis CC. 1948. *Gymnodinium brevis* sp. nov., a cause of discolored water and animal mortality in the Gulf of Mexico. *Bot Gaz* 109:358-60
- Dragovich A, Funicane JH, and May BZ. 1961. Counts of red tide organisms, *Gymnodinium breve*, and associated oceanographic data from Florida west coast, 1957-59. *US Fish Wildl Serv Spec Sci Rep Fish* 369:1-175
- Dragovich A, Funicane JH, Kelly JA, *et al.* 1963. Counts of red tide organisms, *Gymnodinium breve*, and associated oceanographic data from Florida west coast, 1960-61. *US Fish Wildl Serv Spec Sci Rep Fish* 455:1-39
- Fahnenstiel GL, McCormick *et al.* 1995. Taxon-specific growth and loss rates for dominant phytoplankton populations from the northern Gulf of Mexico. *Mar Ecol Progr Ser* 117:229- 39
- Franks P. 1997. Spatial patterns in dense algal blooms. *Limnol Oceanogr* 42:1297-305
- Gilbes F, Tomas C, Walsh JJ, *et al.* 1996. An episodic chlorophyll plume on the west Florida shelf. *Cont Shelf Res* 16:1201-24
- Glibert PM and Bronk DA. 1994. Release of dissolved organic nitrogen by marine diazotrophic cyanobacteria, *Trichodesmium* spp. *Appl Environ Microbiol* 60: 3996-4000
- Gunther G, Williams RH , Davis CC, *et al.* 1948. Catastrophic mass mortality of marine animals and coincident phytoplankton bloom on the west coast of Florida, November 1946 to August 1947. *Ecol Monogr* 18:309-24

- Haddad KD. 1982. Hydrographic Factors Associated with West Florida Toxic Red Tide Blooms: An Assessment for Satellite Prediction and Monitoring. M.S. Thesis, pp 1-155. University of South Florida, Tampa, FL, USA
- Hansen PJ. 1995. Growth and grazing of a ciliate feeding on the red tide dinoflagellate *Gyrodinium aureolum* in monoculture and in mixture with a non-toxic alga. Mar Ecol Progr Ser 121:65-72
- Heil CA. 1986. Vertical Migration of *Ptychodiscus brevis* (Davis) Steidinger. M.S. Thesis, pp 1-118. University of South Florida, Tampa, FL, USA
- Hitchcock GL, Vargo GA, and Dickson ML. 2000. Phytoplankton community composition, production, and respiration in relation to dissolved inorganic carbon on the West Florida shelf, April 1996. J Geophys Res 105:6579-90
- Houde ED and Chitty N. 1976. Seasonal Abundance and Distribution of Zooplankton, Fish Eggs, and Fish Larvae in the Eastern Gulf of Mexico, 1972-74. NOAA Tech. Rep. NMFS SSRF-701, pp 1-12. Seattle, WA, USA
- Huisman J and Weissing FJ. 1999. Biodiversity of plankton by species oscillations and chaos. Nature 402:407-10
- Hutchinson GE. 1961. The paradox of the plankton. Amer Nat 95:137-45
- Joint I, Lewis J, Aiken J, *et al.* Interannual variability of PSP outbreaks on the north east UK coast. 1997. J Plankt Res 19:937-56
- Kamykowski D, Milligan EJ, and Reed RE. 1998. Biochemical relationships with the orientation of the autotrophic dinoflagellate *Gymnodinium breve* under nutrient replete conditions. Mar Ecol Progr Ser 167:105-17
- Kierstead H and Slobodkin LB. 1953. The size of water masses containing plankton blooms. J Mar Res 12:141-7
- Kleppel GS, Burkart CA, Carter K, *et al.* 1996. Diets of calanoid copepods on the West Florida continental shelf: relationships between food concentration, food composition and feeding activity. Mar Biol 127:209-18
- Lenes JM, Darrow BP, Catrall C, *et al.* 2001. Iron fertilization and the *Trichodesmium* response on the West Florida shelf. Limnol Oceanogr 46:1261-1277
- Leonard CL, McClain CR, Murtugudde R, *et al.* 1999. An iron-based ecosystem model of the central equatorial Pacific. J Geophys Res 104:1325-41
- Li Z and Weisberg RH. 1999. West Florida Shelf response to upwelling favorable wind forcing, Part 1: Kinematics. J Geophys Res 104:13,507-27
- Millie DF, Kirkpatrick GJ, and Vinyard BT. 1995. Relating photosynthetic pigments and *in vivo* optical density spectra to irradiance for the Florida red tide dinoflagellate, *Gymnodinium breve*. Mar Ecol Progr Ser 120:65-75
- Millie DF, Schofield OM, Kirkpatrick GJ, *et al.* 1997. Detection of harmful algal blooms using photopigments and absorption signatures: a case study of the Florida red tide dinoflagellate, *Gymnodinium breve*. Limnol Oceanogr 42:1240-51
- Morin PJ. 2000. The complexity of co-dependency. Nature 403:718-9
- Nakamura Y, Suzuki S, and Hiromi J. 1996. Development and collapse of a *Gymnodinium mikimotoi* red tide in the Seto Inland Sea. Aquat Microb Ecol 10:131-7
- Nelson JR, Eckman JE, Robertson CY, *et al.* 1999. Benthic microalgal biomass and irradiance at the sea floor on the continental shelf of the South Atlantic Bight: spatial and temporal variability and storm effects. Cont Shelf Res 19:477-506
- Penta B. 2000. Phytoplankton Competition in the West Florida Shelf: A Simulation Analysis with "Red tide" Implications. Ph.D. dissertation, pp 1-118. University of South Florida, Tampa, FL, USA
- Schofield O, Grzyski J, Bissett WP, *et al.* 1999. Optical monitoring and forecasting systems for harmful algal blooms: possibility or pipe dream? Phycology 35:1477-96



## Ecological Modeling of Harmful Algal Blooms

- Shanley E and Vargo GA. 1993. Cellular composition, growth, photosynthesis, and respiration rates of *Gymnodinium breve* under varying light levels. In: Smayda TJ and Shimizu Y (eds), Toxic Phytoplankton Blooms in the Sea, pp 831-6. Elsevier, Amsterdam, The Netherlands
- Slobodkin LB. 1953. A possible initial condition for red tides on the coast of Florida. J Mar Res 12:148-55
- Steidinger KA, Vargo GA, Tester PA, *et al.* 1998. Bloom dynamics and physiology of *Gymnodinium breve* with emphasis on the Gulf of Mexico. In: Anderson DM, Cembella AD, and Hallegraeff GM (eds), Physiological Ecology of Harmful Algal Blooms, pp 135-53. Springer Verlag, Berlin, Germany
- Strom SL and Strom MW. 1996. Microplankton growth, grazing, and community structure in the northern Gulf of Mexico. Mar Ecol Progr Ser 130:229-40
- Tester PA and Steidinger KA. 1997. *Gymnodinium breve* red tide blooms: initiation, transport, and consequences of surface circulation. Limnol Oceanogr 42:1039-51
- Turner JT and Tester PA. 1997. Toxic marine phytoplankton, zooplankton grazers, and pelagic food webs. Limnol Oceanogr 42:1203-14
- Van Dolah FM and Leighfield TA. 1999. Diel phasing of the cell-cycle in the Florida red tide dinoflagellate, *Gymnodinium breve*. Phycology 35:1404-11
- Vargo GA, Carder KL, Gregg WW, *et al.* 1987. The potential contribution of primary production by red tides to the west Florida shelf ecosystem. Limnol Oceanogr 32:762-6
- Walsh JJ. 1975. A spatial simulation model of the Peru upwelling ecosystem. Deep-Sea Res 22:201-36
- Walsh JJ and Dieterle DA. 1994. CO<sub>2</sub> cycling in the coastal ocean. I. A numerical analysis of the southeastern Bering Sea, with applications to the Chukchi Sea and the northern Gulf of Mexico. Progr Oceanogr 34:335-92
- Walsh JJ and Steidinger KA. 2001. Saharan dust and Florida red tides: the cyanophyte connection. J Geophys Res 106:11597-11612
- Walsh JJ, Dieterle DA, Muller-Karger FE, *et al.* 1999. A numerical simulation of carbon/nitrogen cycling during spring upwelling in the Cariaco Basin. J Geophys Res 104:7807-25
- Walsh JJ, Haddad KD, Dieterle DA, *et al.* 2001a. A numerical analysis of the landfall of 1979 red tide of *Gymnodinium breve* along the west coast of Florida — the fall/winter upwelling mode. Cont Shelf Res (*in press*)
- Walsh JJ, Dieterle DA, and Lenes J. 2001b. A numerical analysis of carbon dynamics of the Southern Ocean phytoplankton community: the roles of light and grazing in effecting both sequestration of atmospheric CO<sub>2</sub> and food availability to larval krill. Deep-Sea Res 48:1-48
- Yanagi T, Yamamoto T, Koizumi Y, *et al.* 1995. A numerical simulation of red tide formation. J Mar Syst 6:269-85
- Yang H and Weisberg RH. 1999. West Florida continental shelf circulation response to climatological wind forcing. J Geophys Res 104:5301-20